Article DOI: https://doi.org/10.3201/eid2812.220572

# Emergence and Evolutionary Response of *Vibrio cholerae* to a Novel Bacteriophage in the Democratic Republic of the Congo

## Appendix

## Materials and Methods

### Isolation and Characterization of Toxigenic *Vibrio cholerae* O1 and Virulent Phages

During 2015–2017, fecal samples from suspected cholera patients admitted in different cholera treatment centers around Goma, Democratic Republic of the Congo (DRC) (Table) were placed on Cary-Blair transport media and brought to the Laboratoire Provincial de Sante Publique du Nord-Kivu in Goma for microbiological and serologic analysis. *V. cholerae* in fecal samples were enriched in alkaline peptone water as described elsewhere (*1*). Following enrichment, a loopful of culture was streaked onto thiosulfate citrate bile salts (TCBS) agar and the plates were incubated overnight at 37°C. Bacterial colonies grown as yellow color on TCBS agar were subcultured onto Luria-Bertani, Miller (LB) agar and the culture plates were incubated overnight at 37°C. To determine serogroup, translucent colonies grown on LB-agar were tested against polyvalent antiserum specific for *V. cholerae* O1 and O139 by slide agglutination tests; each O1 positive strain was further typed for serotype using antiserum specific for Ogawa, Inaba, or Hikojima serotype. The toxigenic *V. cholerae* were stored in soft LB-agar (0.7% agar) and sent to the Emerging Pathogens Institute (EPI) at University of Florida for further analysis.

For isolation of potential virulent phages, cholera rice-water fecal samples collected between 2016 and 2017 were centrifuged at 5,000 x g for 10 min in a microfuge. Fecal samples sused to detect and characterize virulent phages were different than the fecal samples used for detection of 24 *V. cholerae* O1 strains described above. The resultant supernatant was filtered through a 0.22 µm syringe filter, stored at 4°C in a sterile microfuge tube, and sent to EPI for further analysis. For further characterization of potential phages in cholera-confirmed patients' fecal samples, 41 fecal sample filtrates were brought to EPI.

Virulent phage plaque assay: For detection and characterization of potential virulent phages, each filtered fecal sample was tested by plaque assay using a host toxigenic *V. cholera*e O1 Inaba strain, AGC-15 (Appendix Table 1). Isolated in DRC, AGC-15 has a wild-type *ompU* sequence, which encodes the receptor for ICP2. AGC-15 also has the O1-antigen receptor for ICP1 and ICP3 (*2*) and lacks any PLE elements mediating immunity to ICP1. Briefly, a sterile glass tube was inoculated with 100 µl of filtered-sterilized fecal sample (potential source of virulent phage), 9.8 ml of LB-broth, and 100 µl of host *V. cholerae* AGC-15 culture (freshly grown to mid-exponential phase). The culture mixture was incubated overnight at 37°C with aeration to enrich any phages capable of infecting AGC-15. Following incubation, the culture was transferred to a 15 ml conical tube and centrifuged for 10 min at 5,000 x g at 4°C. To eliminate residual bacterial cells, the supernatant was filtered through a 0.22 µm syringe filter and the filtrate was stored at 4°C. The filtered supernatant was serially diluted (10-fold) in LB-broth to reach a dilution of $10^{-5}$ in a 96-well microtiter plate. One hundred µl of AGC-15 culture (grown to a mid-exponential phase) were added to the undiluted and each serially diluted filtrate in the microtiter plate and was incubated at room temperature for 10 min to enable phage adsorption. All 190 µl of each mixture from the microtiter plate was transferred to wells of six-well tissue culture plates.

Three ml of soft LB-agar (0.35% agar) kept at 55°C in a water bath were added to each well of the six-well plate and the plate was gently swirled to mix the bacteria and phage evenly. To allow the agar to solidify, the plate was left for 30 min at room temperature followed by incubation at 37°C for 3–4 hours. After incubation, the plate was visually observed for plaque formation. If no plaques were observed after 4 hours of incubation, the plate was incubated overnight at room temperature to determine if any plaques were formed following extended incubation time. For virulent phage purification, a single clear plaque was picked using a Pasteur pipette into 1 ml of LB-broth and incubated overnight at 4°C to allow phage to diffuse out of the soft agar piece. High titer stocks of purified plaques were made by multiplication in broth culture as described above.

Whole genome mapping and hqSNP calling: Toxigenic *V. cholerae* O1 samples collected were confirmed by serology and PCR (*1*). After subculture, gDNA extraction was performed using the Qiagen DNeasy Blood and Tissue kit. Genomic DNA from all isolates were cultured and extracted from a bacterial pellet. Sample library construction was performed using the

Nextera XT DNA Library Preparation Kit (Illumina, https://www.illumina.com). Whole-genome sequencing on all isolates was performed with the Illumina MiSeq for 500 cycles. Adaptor and raw sequence reads were filtered by length and quality by using the program Trimmomatic (*3*). After quality filtering, Bowtie2 (*4*) was used to map the sequence reads to the reference genome, *V. cholerae* O1 str. N16961 (GenBank Accessions: NC_002505.1 and NC_002506.1) (*5*). After reads were mapped to the reference genome, duplicate reads were marked and realigned using Picard (http://broadinstitute.github.io/picard). The reference-based mapping alignment was then verified and fixed accordingly. Freebayes (Garrison MG, unpub data; https://arxiv.org/abs/1207.3907) was used to create a custom genome-wide SNP calling database (dbSNP) from all isolates in the dataset to perform base quality score recalibration (BQSR), as outlined in GATK's best practice guidelines for germline variation (https://software.broadinstitute.org/gatk/). The newly created variant call format (VCF) file obtained from Freebayes was subsequently filtered only for SNPs. The VCF file was used as a dbSNP for BQSR of the reference-based mapped alignment files; alignment files were then recalibrated and variants calling on the newly recalibrated files performed with Freebayes. The newly created VCF file was filtered only for SNPs and normalized using the program BCFtools (http://www.htslib.org/doc/bcftools.html). Normalization simplifies the represented variants in the VCF file by showing as few bases as possible at particular SNP sites in the genome. SNPs were filtered by depth of coverage, quality, and genotype likelihood, as described in Azarian *et al.* (*6*). Finally, the SNP FASTA alignment was extracted by a custom python script from the VCF file. The SNP alignment was filtered site-by-site, leaving sites with only greater than 75% of SNPs at that particular site, making a high-quality SNP (hqSNP) alignment. Our hqSNP alignment was then annotated using the program SnpEff (*7*). The final genome-wide SNP alignment included 120 T10 sublineage *V. cholerae* genome sequences (Appendix Table 1): 24 strains were collected in DRC (eight collected in 2015, five in 2016, 11 in 2017) and sequenced in this study; 71 were publicly available genomes from outbreaks in eastern DRC between 2014 and 2016 (*8*); six archival and publicly available DRC genomes collected between 2001–2013; 17 genomes collected across Africa between 1998 and 2014; and two publicly available genomes from India, ancestor of T10 sublineage (*9*). While the previously available DRC samples spanned 2014–2016 (*10*), we expanded the temporal dimension of the DRC collection as we sequenced mainly strains collected in 2017. The MLST analysis was performed on the online

tool PubMLST (Jolley K, unpub data; https://doi.org/10.12688/wellcomeopenres.14826.1); results are shown in Appendix Table 2.

Phylogenetic and temporal signal: All datasets used in this study passed phylogenetic quality checks such as evaluating the presence of phylogenetic signal, to resolve the phylogenetic relationship among the *V. cholerae* isolates, and temporal signal for a robust calibration of the molecular clock (Appendix Figure 1). We performed likelihood mapping analysis using IQ-TREE (*10*), which enables the report likelihood values of the three possible unrooted trees, inferred using the best-fitting nucleotide substitution model, of each possible quartet (set of four sequences) on an equilateral triangle (likelihood map). In a likelihood map, dots (likelihood values) in the center of the triangle represent phylogenetic noise and simulation have shown that datasets with <35% nose (as it was in our case) can reliably be used for phylogeny inference (*11*). For each dataset, the presence of temporal signal was assessed by calculating the tree root-to-tip divergence regression plot with TempEst v1.5 (http://tree.bio.ed.ac.uk/software/tempest) (*12*), using maximum-likelihood (ML) phylogenies inferred with IQ-TREE (*10*) and the best-fitting nucleotide substitution model according to Bayesian Information Criterion (BIC), and ultrafast bootstrap (BB) approximation (1000 replicates) to assess robustness of the phylogeny internal branches.

Bayesian Phylogeography of DRC isolates: To test the hypothesis of whether cholera outbreaks in the DRC were caused by endemic *V. cholerae* O1 strains, or strains recently introduced from other African countries surrounding the Great Lakes region, we used the Bayesian phylogeographic (*13*) coalescent-based method (*14*) implemented in the BEAST v1.10.4 (*15*) software package. The reconstruction of *V. cholerae* O1 spatiotemporal spread from different locations through Bayesian phylogeography requires the calibration of a molecular clock. Evolutionary rates were estimated implementing a HKY nucleotide substitution model (*16*) with empirical base frequencies, gamma distribution of site-specific rate heterogeneity, and ascertainment bias correction (*17*), testing a constant demographic prior against non-parametric demographic models – Gaussian Markov randomfield Skyride (BSR) (*18*) and Bayesian Skyline Plot (BSP) (*19*) – to rule out spurious changes in effective population size inferred by a non-parametric model that would in turn effect timing of divergence events (*20*). Additionally, for each demographic model, we compared a strict and relaxed uncorrelated (lognormal distribution among branches) molecular clock (*21*). The best fitting molecular clock and demographic model

were chosen by estimating the marginal likelihood of each model by using path sampling (PS) and stepping-stone (SS) methods, followed by Bayes Factor comparison test (*11*,*15*). A Markov Chain Monte Carlo (MCMC) sampler was run for 500 million generations, sampling every 50,000 generations. Proper mixing of the Markov chain was evaluated by the effective population size (ESS) of each parameter estimate under a specific model. ESS values >200 for all parameter estimates are considered as evidence of proper mixing in the analysis. The sampling location for each isolate was used as a discreet trait to reconstruct likely locations of ancestral sequences (internal nodes in the tree) and infer migration events (bacterial flow) that took place in the DRC and throughout the Great Lakes Region. Phylogeographic analysis was performed with the BEAST package v1.10.4 (*15*). Transitions between discrete states (location of where the isolate was collected) were estimated using the continuous-time Markov chain model operating the asymmetric migration model with Bayesian Stochastic Search Variable Selection (*13*). In our reconstruction of ancestral states, we assume migration occurs along branches connecting the tree nodes. The maximum clade credibility (MCC) tree chosen from the posterior distribution of trees using TreeAnnotator v1.10.4 after 10% burn-in. The MCC tree was annotated in R using the package ggtree (*22*) for publishing purposes.

Calculation of weighted average of nonsynonmous (*dN*) and synonymous substitution rates (*dS*), and selection analysis: A codon alignment from the DRC clade was generated to analyze other mutations in the *V. cholerae* genome from the isolates in the phylogeny, and a subset of 200 Bayesian MCC genealogies randomly was obtained from the posterior distribution of trees for each subsampled dataset. The weighted average of synonymous substitution rates (*dS*) and non-synonymous substitution rates (*dN*) in the protein-coding regions of the *V. cholerae* O1 genome for all, internal and external branches were obtained from a subset of 200 Bayesian MCC trees randomly obtained from the posterior distribution of trees, as described by Lemey et al. (*23*). The subset of trees and in-house java scripts were then used to calculate *dN/dS* rates and divergence in the isolates located within the DRC clade and plotted using the package ggplot2 in R.

**Whole genome sequencing, genome assembly and annotation of DRC phages**

To characterize DRC phages, we plaque-purified phages from eight different patient samples, and prepared high titer stocks of each of these phages. Sample library construction for whole-genome sequencing was performed using the Nextera XT DNA Library Preparation Kit

(Illumina). Whole-genome sequencing was performed with the Illumina MiSeq for 50 cycles. We obtained over 200-fold coverage facilitating de novo assembly of each phage genome into one complete contig using CLC Genomics Workbench (QIAGEN, https://www.qiagen.com). Manual confirmation/correction of low coverage areas and/or problem areas were performed to ensure authentic genome assembly. Annotation of phage genomes was performed as described elsewhere (*24*). Briefly, open reading frames from existing annotated ICP1 phages were compared against the DRC phage genomes using BLASTn to find homologs. Additional new putative open reading frames were discovered with de novo prediction software and added to the annotation. This was performed for each of the eight phages and due to very high similarity between them, one representative was randomly chosen and designated as ICP1_2017_A_DRC. This representative was aligned with existing ICP1 phage genomes using Mauve (*25*) and a maximum-likelihood, bootstrapped phylogenetic tree was generated with PhyML (-s BEST 92–rand_start–n_rand_starts 10 -b 100) (*26*).

**References**


1. Ali A, Chen Y, Johnson JA, Redden E, Mayette Y, Rashid MH, et al. Recent clonal origin of cholera in Haiti. Emerg Infect Dis. 2011;17:699–701. PubMed https://doi.org/10.3201/eid1704.101973

2. Seed KD, Bodi KL, Kropinski AM, Ackermann HW, Calderwood SB, Qadri F, et al. Evidence of a dominant lineage of *Vibrio cholerae*-specific lytic bacteriophages shed by cholera patients over a 10-year period in Dhaka, Bangladesh. MBio. 2011;2:e00334–10. PubMed https://doi.org/10.1128/mBio.00334-10

3. Bolger AM, Lohse M, Usadel B. Trimmomatic: a flexible trimmer for Illumina sequence data. Bioinformatics. 2014;30:2114–20. PubMed https://doi.org/10.1093/bioinformatics/btu170

4. Langmead B, Salzberg SL. Fast gapped-read alignment with Bowtie 2. Nat Methods. 2012;9:357–9. PubMed https://doi.org/10.1038/nmeth.1923

5. Heidelberg JF, Eisen JA, Nelson WC, Clayton RA, Gwinn ML, Dodson RJ, et al. DNA sequence of both chromosomes of the cholera pathogen *Vibrio cholerae.* Nature. 2000;406:477–83. PubMed https://doi.org/10.1038/35020000

6. Azarian T, Ali A, Johnson JA, Mohr D, Prosperi M, Veras NM, et al. Phylodynamic analysis of clinical and environmental *Vibrio cholerae* isolates from Haiti reveals diversification driven by positive selection. MBio. 2014;5:5. PubMed https://doi.org/10.1128/mBio.01824-14

7. Cingolani P, Platts A, Wang L, Coon M, Nguyen T, Wang L, et al. A program for annotating and predicting the effects of single nucleotide polymorphisms, SnpEff: SNPs in the genome of *Drosophila melanogaster* strain w1118; iso-2; iso-3. Fly (Austin). 2012;6:80–92. PubMed https://doi.org/10.4161/fly.19695

8. Irenge LM, Ambroise J, Mitangala PN, Bearzatto B, Kabangwa RKS, Durant JF, et al. Genomic analysis of pathogenic isolates of Vibrio cholerae from eastern Democratic Republic of the Congo (2014-2017). PLoS Negl Trop Dis. 2020;14:e0007642. PubMed https://doi.org/10.1371/journal.pntd.0007642

9. Weill FX, Domman D, Njamkepo E, Tarr C, Rauzier J, Fawal N, et al. Genomic history of the seventh pandemic of cholera in Africa. Science. 2017;358:785–9. PubMed https://doi.org/10.1126/science.aad5901

10. Nguyen LT, Schmidt HA, von Haeseler A, Minh BQ. IQ-TREE: a fast and effective stochastic algorithm for estimating maximum-likelihood phylogenies. Mol Biol Evol. 2015;32:268–74. PubMed https://doi.org/10.1093/molbev/msu300

11. Schmidt HA, Strimmer K, Vingron M, von Haeseler A. TREE-PUZZLE: maximum likelihood phylogenetic analysis using quartets and parallel computing. Bioinformatics. 2002;18:502–4. PubMed https://doi.org/10.1093/bioinformatics/18.3.502

12. Rambaut A, Lam TT, Max Carvalho L, Pybus OG. Exploring the temporal structure of heterochronous sequences using TempEst (formerly Path-O-Gen). Virus Evol. 2016;2:vew007. PubMed https://doi.org/10.1093/ve/vew007

13. Lemey P, Rambaut A, Drummond AJ, Suchard MA. Bayesian phylogeography finds its roots. PLOS Comput Biol. 2009;5:e1000520. PubMed https://doi.org/10.1371/journal.pcbi.1000520

14. Grenfell BT, Pybus OG, Gog JR, Wood JL, Daly JM, Mumford JA, et al. Unifying the epidemiological and evolutionary dynamics of pathogens. Science. 2004;303:327–32. PubMed https://doi.org/10.1126/science.1090727

15. Drummond AJ, Rambaut A. BEAST: Bayesian evolutionary analysis by sampling trees. BMC Evol Biol. 2007;7:214. PubMed https://doi.org/10.1186/1471-2148-7-214

16. Hasegawa M, Kishino H, Yano T. Dating of the human-ape splitting by a molecular clock of mitochondrial DNA. J Mol Evol. 1985;22:160–74. PubMed https://doi.org/10.1007/BF02101694

17. Leaché AD, Banbury BL, Felsenstein J, de Oca AN, Stamatakis A. Short tree, long tree, right tree, wrong tree: new acquisition bias corrections for inferring SNP phylogenies. Syst Biol. 2015;64:1032–47. PubMed https://doi.org/10.1093/sysbio/syv053

18. Minin VN, Bloomquist EW, Suchard MA. Smooth skyride through a rough skyline: Bayesian coalescent-based inference of population dynamics. Mol Biol Evol. 2008;25:1459–71. PubMed https://doi.org/10.1093/molbev/msn090

19. Strimmer K, Pybus OG. Exploring the demographic history of DNA sequences using the generalized skyline plot. Mol Biol Evol. 2001;18:2298–305. PubMed https://doi.org/10.1093/oxfordjournals.molbev.a003776

20. Hall MD, Woolhouse ME, Rambaut A. The effects of sampling strategy on the quality of reconstruction of viral population dynamics using Bayesian skyline family coalescent methods: A simulation study. Virus Evol. 2016;2:vew003. PubMed https://doi.org/10.1093/ve/vew003

21. Drummond AJ, Rambaut A, Shapiro B, Pybus OG. Bayesian coalescent inference of past population dynamics from molecular sequences. Mol Biol Evol. 2005;22:1185–92. PubMed https://doi.org/10.1093/molbev/msi103

22. Yu GC, Smith DK, Zhu HC, Guan Y, Lam TTY. GGTREE: an R package for visualization and annotation of phylogenetic trees with their covariates and other associated data. Methods Ecol Evol. 2017;8:28–36. https://doi.org/10.1111/2041-210X.12628

23. Lemey P, Kosakovsky Pond SL, Drummond AJ, Pybus OG, Shapiro B, Barroso H, et al. Synonymous substitution rates predict HIV disease progression as a result of underlying replication dynamics. PLOS Comput Biol. 2007;3:e29. PubMed https://doi.org/10.1371/journal.pcbi.0030029

24. Angermeyer A, Das MM, Singh DV, Seed KD. Analysis of 19 highly conserved *Vibrio cholerae* bacteriophages isolated from environmental and patient sources over a twelve-year period. Viruses. 2018;10:10. PubMed https://doi.org/10.3390/v10060299

25. Darling AE, Mau B, Perna NT. progressiveMauve: multiple genome alignment with gene gain, loss and rearrangement. PLoS One. 2010;5:e11147. PubMed https://doi.org/10.1371/journal.pone.0011147

26. Guindon S, Dufayard JF, Lefort V, Anisimova M, Hordijk W, Gascuel O. New algorithms and methods to estimate maximum-likelihood phylogenies: assessing the performance of PhyML 3.0. Syst Biol. 2010;59:307–21. PubMed https://doi.org/10.1093/sysbio/syq010

**Appendix Table 1.** *Vibrio cholera* strains included in phylogenetic studies in Democratic Republic of the Congo*

| *V. cholera* name | Year | Location, country or sea | Location, region/ locality | Lineage | Latitude | Longitude | Location on map† | SRA ID |
|---|---|---|---|---|---|---|---|---|
| AGC_1_CD_2015 | 2015 | DRC | North Kivu/ Kirotshe | ST515 | −1.613051 | 29.03132 | 6 | SRR15192533 |
| AGC_2_CD_2015 | 2015 | DRC | Goma/ Buhimba | ST69 | −1.621214 | 29.156623 | 7 | SRR15192532 |
| AGC_3_CD_2015 | 2015 | DRC | Mutwanga | ST515 | 0.514939 | 25.191932 | 8 | SRR15192521 |
| AGC_4_CD_2015 | 2015 | DRC | Goma/ Buhimba | ST515 | −1.621214 | 29.156623 | 7 | SRR15192516 |
| AGC_5_CD_2015 | 2015 | DRC | Goma/ Buhimba | ST515 | −1.621214 | 29.156623 | 7 | SRR15192515 |
| AGC_6_CD_2015 | 2015 | DRC | Goma/ Buhimba | ST515 | −1.621214 | 29.156623 | 7 | SRR15192514 |
| AGC_7_CD_2015 | 2015 | DRC | Goma/ Buhimba | ST515 | −1.621214 | 29.156623 | 7 | SRR15192513 |
| AGC_8_CD_2015 | 2015 | DRC | Goma/ Buhimba | ST515 | −1.621214 | 29.156623 | 7 | SRR15192512 |
| AGC_9_CD_2016 | 2016 | DRC | Maniema/ Kabambare | ST515 | −4.400901 | 27.765835 | 9 | SRR15192511 |
| AGC_10_CD_2016 | 2016 | DRC | Karisimbi/ Hop Millitaire | ST515 | 1.5064 | 29.4508 | 10 | SRR15192510 |
| AGC_11_CD_2016 | 2016 | DRC | Alimbongo | ST515 | −0.36879 | 29.156179 | 11 | SRR15192531 |
| AGC_12_CD_2016 | 2016 | DRC | South Kivu/ Fizi | ST515 | −4.30058 | 28.94212 | 12 | SRR15192530 |
| AGC_13_CD_2016 | 2016 | DRC | South Kivu/ Kimbilulenge | ST515 | −3.21838 | 28.25855 | 13 | SRR15192529 |
| AGC_14_CD_2017 | 2017 | DRC | Kirotshe/ Rubaya | ST515 | −1.546277 | 28.873122 | 14 | SRR15192528 |
| AGC_15_CD_2017 | 2017 | DRC | Rutshuru/ Hgr | ST515 | −1.188054595 | 29.4459123 | 15 | SRR15192527 |
| AGC_16_CD_2017 | 2017 | DRC | Rutshuru/ Hgr | ST515 | −1.188054595 | 29.4459123 | 15 | SRR15192526 |
| AGC_17_CD_2017 | 2017 | DRC | Nyiragongo/ Turunga | ST515 | −1.3527161 | 29.37873 | 16 | SRR15192525 |
| AGC_18_CD_2017 | 2017 | DRC | Goma/Hop Provincial | ST515 | −1.678865426 | 29.8 | 17 | SRR15192524 |
| AGC_19_CD_2017 | 2017 | DRC | Goma/Hop Provincial | ST515 | −1.678865426 | 29.8 | 17 | SRR15192523 |
| AGC_20_CD_2017 | 2017 | DRC | Goma/Hop Provincial | ST515 | −1.678865426 | 29.8 | 17 | SRR15192522 |
| AGC_21_CD_2017 | 2017 | DRC | Karisimbi/ Prison centrale | ST69 | −1.9 | 29 | 18 | SRR15192520 |
| AGC_22_CD_2017 | 2017 | DRC | Karisimbi/ Majengo | ST69 | −1.65388 | 29.5 | 19 | SRR15192519 |
| AGC_23_CD_2017 | 2017 | DRC | Karisimbi/ Majengo | ST515 | −1.65388 | 29.5 | 19 | SRR15192518 |
| AGC_24_CD_2017 | 2017 | DRC | Karisimbi/ Majengo | ST515 | −1.65388 | 29.5 | 19 | SRR15192517 |
| ERR019292_KE_2007 | 2007 | Kenya | | | | | | ERR019292 |
| ERR037738_KE_2010 | 2010 | Kenya | | | | | | ERR037738 |
| ERR044795_ZM_2003 | 2003 | Zambia | | | | | | ERR044795 |
| ERR1877642_RW_2000 | 2000 | Rwanda | | | | | | ERR1877642 |
| ERR1878097_CD_2003 | 2003 | DRC | | | | | | ERR1878097 |
| ERR1878101_CD_2002 | 2002 | DRC | Congo/ Zaire | | −11.64112 | 27.51818 | 3 | ERR1878101 |
| ERR1878103_KM_2003 | 2003 | Comoros | | | | | | ERR1878103 |
| ERR1878154_KE_2006 | 2006 | Kenya | | | | | | ERR1878154 |
| ERR1878551_DJ_2007 | 2007 | Djibouti | | | | | | ERR1878551 |
| ERR1879386_TZ_1998 | 1998 | Tanzania | | | | | | ERR1879386 |
| ERR1879540_KE_1998 | 1998 | Kenya | | | | | | ERR1879540 |

| *V. cholera* name | Year | Location, country or sea | Location, region/ locality | Lineage | Latitude | Longitude | Location on map† | SRA ID |
|---|---|---|---|---|---|---|---|---|
| ERR1880767_TZ_1998 | 1998 | Tanzania | | | | | | ERR1880767 |
| ERR1880801_IN_1997 | 1997 | India | | | | | | ERR1880801 |
| ERR1880812_IN_1998 | 1998 | India | | | | | | ERR1880812 |
| ERR2265670_NE_2014 | 2014 | Niger | | | | | | ERR2265670 |
| ERR3268992_CD_2017 | 2017 | DRC | Minova | | −4.32153 | 15.31185 | 3 | ERR3268992 |
| ERR3268993_CD_2015 | 2015 | DRC | Goma | | −1.6835 | 29.2356 | 17 | ERR3268993 |
| ERR3268994_CD_2015 | 2015 | DRC | Goma | | −1.6835 | 29.2356 | 17 | ERR3268994 |
| ERR3268995_CD_2015 | 2015 | DRC | Goma | | −1.6835 | 29.2356 | 17 | ERR3268995 |
| ERR3268996_CD_2015 | 2015 | DRC | Goma | | −1.6835 | 29.2356 | 17 | ERR3268996 |
| ERR3268997_CD_2015 | 2015 | DRC | Goma | | −1.6835 | 29.2356 | 17 | ERR3268997 |
| ERR3268998_CD_2015 | 2015 | DRC | Goma | | −1.6835 | 29.2356 | 17 | ERR3268998 |
| ERR3268999_CD_2015 | 2015 | DRC | Goma | | −1.6835 | 29.2356 | 17 | ERR3268999 |
| ERR3269000_CD_2015 | 2015 | DRC | Goma | | −1.6835 | 29.2356 | 17 | ERR3269000 |
| ERR3269001_CD_2015 | 2015 | DRC | Goma | | −1.6835 | 29.2356 | 17 | ERR3269001 |
| ERR3269002_CD_2015 | 2015 | DRC | Goma | | −1.6835 | 29.2356 | 17 | ERR3269002 |
| ERR3269003_CD_2015 | 2015 | DRC | Goma | | −1.6835 | 29.2356 | 17 | ERR3269003 |
| ERR3269004_CD_2015 | 2015 | DRC | Goma | | −1.6835 | 29.2356 | 17 | ERR3269004 |
| ERR3269005_CD_2015 | 2015 | DRC | Goma | | −1.6835 | 29.2356 | 17 | ERR3269005 |
| ERR3269006_CD_2015 | 2015 | DRC | Goma | ST515 | −1.6835 | 29.2356 | 17 | ERR3269006 |
| ERR3269007_CD_2015 | 2015 | DRC | Fizi-Baraka | ST515 | −4.30058 | 28.94212 | 12 | ERR3269007 |
| ERR3269008_CD_2015 | 2015 | DRC | Fizi-Baraka | ST515 | −4.30058 | 28.94212 | 12 | ERR3269008 |
| ERR3269009_CD_2015 | 2015 | DRC | Fizi-Baraka | ST515 | −4.30058 | 28.94212 | 12 | ERR3269009 |
| ERR3269010_CD_2015 | 2015 | DRC | Fizi-Baraka | ST515 | −4.30058 | 28.94212 | 12 | ERR3269010 |
| ERR3269011_CD_2015 | 2015 | DRC | Bukavu | ST515 | −2.50316 | 28.85309 | 21 | ERR3269011 |
| ERR3269012_CD_2015 | 2015 | DRC | Fizi-Baraka | ST515 | −4.30058 | 28.94212 | 12 | ERR3269012 |
| ERR3269013_CD_2015 | 2015 | DRC | Minova | ST515 | −4.32153 | 15.31185 | 3 | ERR3269013 |
| ERR3269014_CD_2016 | 2016 | DRC | Fizi-Baraka | ST515 | −4.30058 | 28.94212 | 12 | ERR3269014 |
| ERR3269015_CD_2016 | 2016 | DRC | Fizi-Baraka | ST515 | −4.30058 | 28.94212 | 12 | ERR3269015 |
| ERR3269016_CD_2016 | 2016 | DRC | Fizi-Baraka | ST515 | −4.30058 | 28.94212 | 12 | ERR3269016 |
| ERR3269017_CD_2016 | 2016 | DRC | Fizi-Baraka | ST515 | −4.30058 | 28.94212 | 12 | ERR3269017 |
| ERR3269018_CD_2016 | 2016 | DRC | Fizi-Baraka | ST515 | −4.30058 | 28.94212 | 12 | ERR3269018 |
| ERR3269019_CD_2016 | 2016 | DRC | Fizi-Baraka | ST515 | −4.30058 | 28.94212 | 12 | ERR3269019 |
| ERR3269020_CD_2016 | 2016 | DRC | Uvira | ST515 | −3.38413 | 29.1415 | 20 | ERR3269020 |
| ERR3269021_CD_2016 | 2016 | DRC | Uvira | ST515 | −3.38413 | 29.1415 | 20 | ERR3269021 |

| *V. cholera* name | Year | Location, country or sea | Location, region/ locality | Lineage | Latitude | Longitude | Location on map† | SRA ID |
|---|---|---|---|---|---|---|---|---|
| ERR3269022_CD_2016 | 2016 | DRC | Uvira | ST69 | −3.38413 | 29.1415 | 20 | ERR3269022 |
| ERR3269023_CD_2016 | 2016 | DRC | Uvira | ST69 | −3.38413 | 29.1415 | 20 | ERR3269023 |
| ERR3269024_CD_2016 | 2016 | DRC | Uvira | ST69 | −3.38413 | 29.1415 | 20 | ERR3269024 |
| ERR3269025_CD_2016 | 2016 | DRC | Uvira | ST69 | −3.38413 | 29.1415 | 20 | ERR3269025 |
| ERR3269026_CD_2016 | 2016 | DRC | Uvira | ST515 | −3.38413 | 29.1415 | 20 | ERR3269026 |
| ERR3269027_CD_2016 | 2016 | DRC | Fizi-Baraka | ST69 | −4.30058 | 28.94212 | 12 | ERR3269027 |
| ERR3269028_CD_2015 | 2015 | DRC | Fizi-Baraka | ST515 | −4.30058 | 28.94212 | 12 | ERR3269028 |
| ERR3269029_CD_2015 | 2015 | DRC | Fizi-Baraka | ST515 | −4.30058 | 28.94212 | 12 | ERR3269029 |
| ERR3269031_CD_2016 | 2016 | DRC | Alimbongo | ST515 | −0.3692 | 29.155569 | 8 | ERR3269031 |
| ERR3269033_CD_2016 | 2016 | DRC | Kabambare | ST69 | −4.68967 | 27.69298 | 9 | ERR3269033 |
| ERR3269034_CD_2016 | 2016 | DRC | Fizi-Baraka | ST69 | −4.30058 | 28.94212 | 12 | ERR3269034 |
| ERR3269035_CD_2016 | 2016 | DRC | Fizi-Baraka | ST515 | −4.30058 | 28.94212 | 12 | ERR3269035 |
| ERR3269036_CD_2016 | 2016 | DRC | Fizi-Baraka | ST69 | −4.30058 | 28.94212 | 12 | ERR3269036 |
| ERR3269037_CD_2016 | 2016 | DRC | Kimbilulenge | ST69 | −4.32153 | 15.31185 | 3 | ERR3269037 |
| ERR3269038_CD_2016 | 2016 | DRC | Kimbilulenge | ST69 | −4.32153 | 15.31185 | 3 | ERR3269038 |
| ERR3269039_CD_2014 | 2014 | DRC | Fizi-Baraka | ST69 | −4.30058 | 28.94212 | 12 | ERR3269039 |
| ERR3269040_CD_2014 | 2014 | DRC | Fizi-Baraka | ST69 | −4.30058 | 28.94212 | 12 | ERR3269040 |
| ERR3269041_CD_2014 | 2014 | DRC | Fizi-Baraka | ST69 | −4.30058 | 28.94212 | 12 | ERR3269041 |
| ERR3269042_CD_2014 | 2014 | DRC | Alimbongo | ST69 | −0.3692 | 29.155569 | 8 | ERR3269042 |
| ERR3269043_CD_2015 | 2015 | DRC | Masisi | ST69 | −1.3527161 | 29.37873 | 16 | ERR3269043 |
| ERR3269044_CD_2014 | 2014 | DRC | Fizi-Baraka | ST69 | −4.30058 | 28.94212 | 12 | ERR3269044 |
| ERR3269045_CD_2014 | 2014 | DRC | Fizi-Baraka | ST69 | −4.30058 | 28.94212 | 12 | ERR3269045 |
| ERR3269047_CD_2015 | 2015 | DRC | Goma | ST69 | −1.6835 | 29.2356 | 17 | ERR3269047 |
| ERR3269048_CD_2015 | 2015 | DRC | Goma | ST515 | −1.6835 | 29.2356 | 17 | ERR3269048 |
| ERR3269049_CD_2015 | 2015 | DRC | Goma | ST69 | −1.6835 | 29.2356 | 17 | ERR3269049 |
| ERR3269050_CD_2015 | 2015 | DRC | Goma | ST69 | −1.6835 | 29.2356 | 17 | ERR3269050 |
| ERR3269051_CD_2014 | 2014 | DRC | Uvira | ST69 | −3.38413 | 29.1415 | 20 | ERR3269051 |
| ERR3269052_CD_2014 | 2014 | DRC | Uvira | ST69 | −3.38413 | 29.1415 | 20 | ERR3269052 |
| ERR3269053_CD_2014 | 2014 | DRC | Uvira | ST69 | −3.38413 | 29.1415 | 20 | ERR3269053 |
| ERR3269054_CD_2014 | 2014 | DRC | Uvira | ST69 | −3.38413 | 29.1415 | 20 | ERR3269054 |
| ERR3269056_CD_2014 | 2014 | DRC | Uvira | ST515 | −3.38413 | 29.1415 | 20 | ERR3269056 |
| ERR3269057_CD_2014 | 2014 | DRC | Fizi-Baraka | ST515 | −4.30058 | 28.94212 | 12 | ERR3269057 |
| ERR3269058_CD_2014 | 2014 | DRC | Fizi-Baraka | ST69 | −4.30058 | 28.94212 | 12 | ERR3269058 |

| *V. cholera* name | Year | Location, country or sea | Location, region/ locality | Lineage | Latitude | Longitude | Location on map† | SRA ID |
|---|---|---|---|---|---|---|---|---|
| ERR3269059_CD_2014 | 2014 | DRC | Goma | ST515 | −1.6835 | 29.2356 | 17 | ERR3269059 |
| ERR3269060_CD_2014 | 2014 | DRC | Fizi-Baraka | ST515 | −4.30058 | 28.94212 | 12 | ERR3269060 |
| ERR3269061_CD_2014 | 2014 | DRC | Fizi-Baraka | ST69 | −4.30058 | 28.94212 | 12 | ERR3269061 |
| ERR3269062_CD_2014 | 2014 | DRC | Goma | ST69 | −1.6835 | 29.2356 | 17 | ERR3269062 |
| ERR3269063_CD_2014 | 2014 | DRC | Fizi-Baraka | ST613 | −4.30058 | 28.94212 | 12 | ERR3269063 |
| ERR3269064_CD_2014 | 2014 | DRC | Fizi-Baraka | ST612 | −4.30058 | 28.94212 | 12 | ERR3269064 |
| ERR3269065_CD_2015 | 2015 | DRC | Goma | ST515 | −1.6835 | 29.2356 | 17 | ERR3269065 |
| ERR3269066_CD_2015 | 2015 | DRC | Goma | ST515 | −1.6835 | 29.2356 | 17 | ERR3269066 |
| ERR386629_CD_2009 | 2009 | DRC | | | −5.91312 | 29.20005 | 4 | ERR386629 |
| ERR386661_ZM_2012 | 2012 | DRC | | | | | | ERR386661 |
| ERR386712_CD_2012 | 2012 | DRC | Biyela | ST515 | −4.32153 | 15.31185 | 5 | ERR386712 |
| ERR572559_CD_2013 | 2013 | DRC | Nyemba | ST69 | −8.16966 | 25.38507 | 1 | ERR572559 |
| ERR572810_CD_2001 | 2001 | DRC | Ankoro | | −6.75053 | 26.94274 | 2 | ERR572810 |
| ERR976553_UG_1998 | 1998 | Uganda | | | | | | ERR976553 |
| ERR976558_KM_1998 | 1998 | Comoros | | | | | | ERR976558 |
| ERR976569_RW_1998 | 1998 | Rwanda | | | | | | ERR976569 |
| ERR976575_SD_1998 | 1998 | Sudan | | | | | | ERR976575 |
| ERR976593_MG_2000 | 2000 | Madagascar | | | | | | ERR976593 |

*DRC, Democratic Republic of the Congo.
†Map in Figure 1.

**Appendix Table 2.** Results of MLST analysis of DRC *V. cholerae* strains

| Sample name | MLST profile (ST) |
|---|---|
| AGC_12_CD_2016 | 69 |
| AGC_13_CD_2016 | 69 |
| AGC_9_CD_2016 | 69 |
| AGC_1_CD_2015 | 515 |
| AGC_10_CD_2016 | 515 |
| AGC_11_CD_2016 | 515 |
| AGC_14_CD_2017 | 515 |
| AGC_15_CD_2017 | 515 |
| AGC_16_CD_2017 | 515 |
| AGC_17_CD_2017 | 515 |
| AGC_18_CD_2017 | 515 |
| AGC_19_CD_2017 | 515 |
| AGC_2_CD_2015 | 515 |
| AGC_20_CD_2017 | 515 |
| AGC_21_CD_2017 | 515 |
| AGC_22_CD_2017 | 515 |
| AGC_23_CD_2017 | 515 |
| AGC_24_CD_2017 | 515 |
| AGC_3_CD_2015 | 515 |
| AGC_4_CD_2015 | 515 |
| AGC_5_CD_2015 | 515 |
| AGC_6_CD_2015 | 515 |
| AGC_7_CD_2015 | 515 |
| AGC_8_CD_2015 | 515 |

**Appendix Table 3.** ICP1 phage which were sequenced

| Strain | Isolation date | Province/Location | SRA ID |
|---|---|---|---|
| DRC32 | 1/11/2017 | Rutshuru/Hgr | SRR18305671 |
| DRC48 | 3/18/2017 | Goma/Hgr | SRR18305670 |
| DRC55 | 3/30/2017 | Rutshuru/Tongo | SRR18305669 |
| DRC72 | 3/2/2017 | Kirotshe/Sake | SRR18305668 |
| DRC74 | 3/2/2017 | Kirotshe/Sake | SRR18305667 |
| DRC82 | 4/11/2017 | Rutshuru/Ntamugenga | SRR18305666 |
| DRC87 | 4/15/2017 | Nyiragongo/Kibumba | SRR18305665 |
| DRC106 | 4/22/2017 | Kibumba | SRR18305664 |

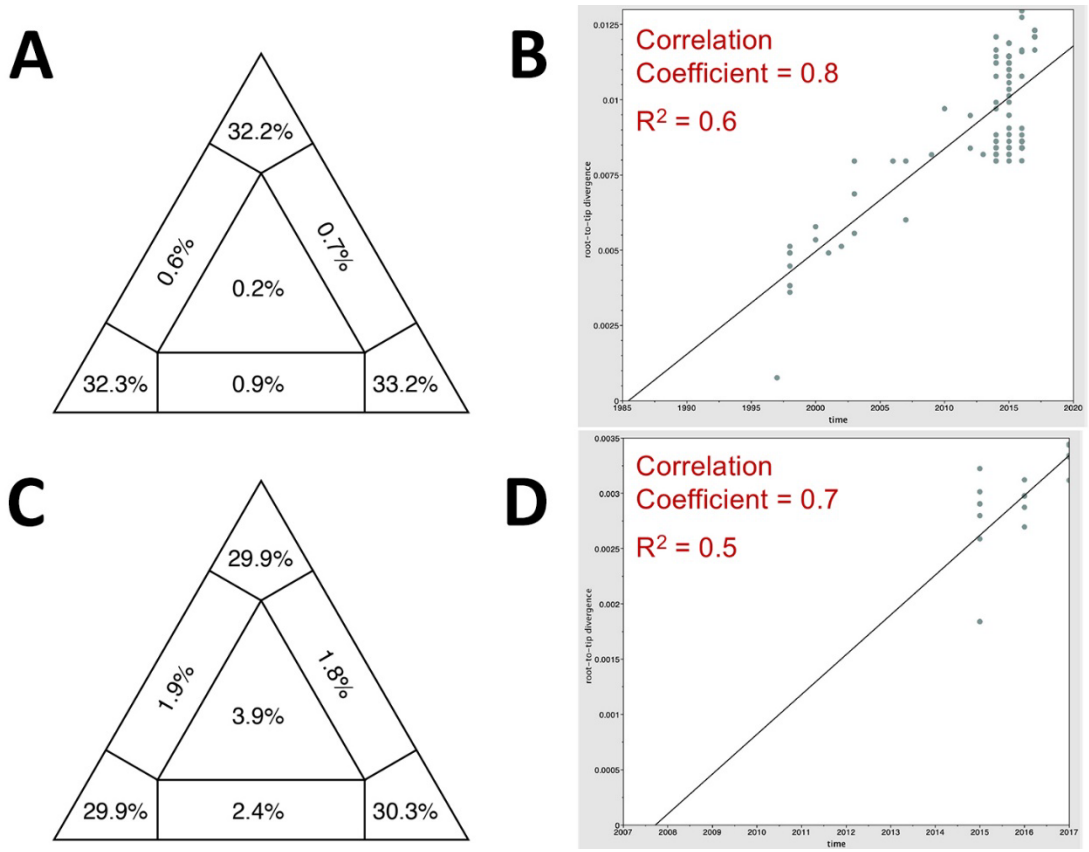


**Appendix Figure 1.** Estimations of phylogenetic and temporal signal from the DRC phylogenies. Presence of phylogenetic signal in the dataset of the *V. cholerae* A) dataset displayed in Figure 1 (isolates collected by our group and downloaded from NCBI), as well as C) the dataset displayed in Figure 3 (isolates collected by our group only), was evaluated by likelihood mapping check for alternative topologies (tips), unresolved quartets (center) and partly resolved quartets (edges) for each dataset. Linear regressions of root-to-tip genetic distance within the ML phylogeny (tree in Figure 1) against sampling time for each taxon. Temporal resolution for B) dataset displayed Figure 1 or D) dataset displayed in Figure 3 was assessed using the slope of the regression, with positive slope indicating sufficient temporal signal. Correlation coefficient, r, and $R^2$ are reported in the temporal signal plot.

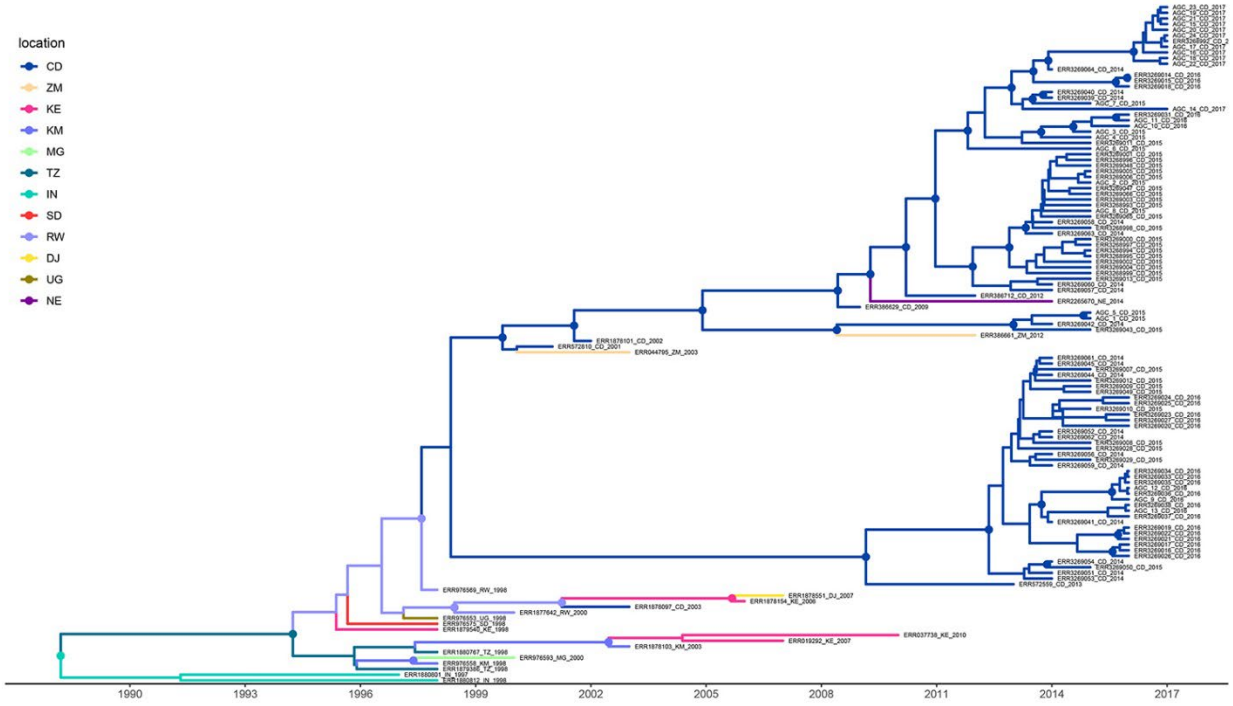


**Appendix Figure 2.** MCC in Figure 1 tree with tips. Phylogeny reported in Figure 1 with tips. Branches of the phylogeny are scaled in time and colored by country of origin as shown in the legend (location). Circles in internal node indicate posterior probability support >0.9 and the colors indicate the ancestral country inferred by Bayesian phylogeography reconstruction. CD, Democratic Republic of Congo; ZM, Zambia; KE, Kenya; KM, Comoros; MG, Kyrgyzstan; TZ, United Republic of Tanzania; IN, India; SD, Sudan; RW, Rwanda; DJ, Djibouti; UG, Uganda; NE, Niger

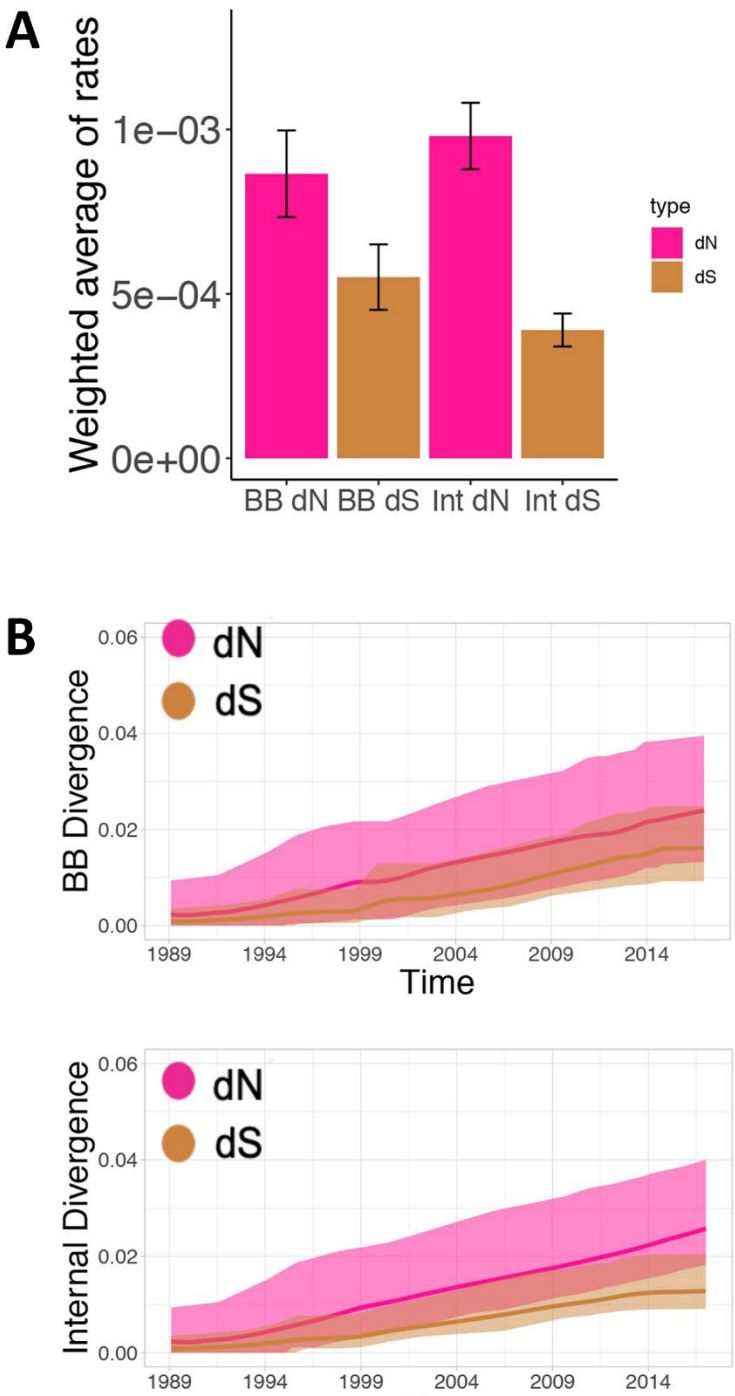


**Appendix Figure 3.** Tree, synonymous and nonsynonymous substitution rates. A) Weighted average of synonymous and nonsynonymous substitution rates of backbone and internal branches based on the Bayesian phylogeography tree in Figure 1. B) Absolute synonymous (tan) and nonsynonymous (pink) divergence rates (y-axis) against time in years (x-axis) of backbone (top) and internal branches (bottom) of the phylogeny. BB, backbone; dN, nonsynonymous substitution rates; dS, synonymous substitution rates